Research article

Clinical and biological underpinnings of longitudinal atrophy pattern progression in Alzheimer's disease

Journal of Alzheimer's Disease
1–13

DOI: 10.1177/13872877241299843
journals.sagepub.com/home/alz

Pilar M. Ferraro[1,*], Laura Filippi[1,*], Marta Ponzano[2], Alessio Signori[2], Beatrice Orso[3], Federico Massa[1,3], Dario Arnaldi[1,3], Stefano Caneva[3], Lucia Argenti[3], Mattia Losa[3], Lorenzo Lombardo[3], Pietro Mattioli[1,3], Mauro Costagli[3], Lorenzo Gualco[1], Martina Pulze[1], Domenico Plantone[4], Andrea Brugnolo[1,3], Nicola Girtler[1,3], Andrea Diociasi[2], Sara Garbarino[1], Flavio Villani[1], Maria Pia Sormani[2], Antonio Uccelli[1,3], Luca Roccatagliata[1,2,*], Matteo Pardini[1,3,#] and for the Alzheimer's Disease Neuroimaging Initiative[§]

Abstract

Background: Magnetic resonance imaging (MRI) has recently enabled to identify four distinct Alzheimer's disease (AD) subtypes: hippocampal sparing (HpSp), typical AD (tAD), limbic predominant (Lp), and minimal atrophy (MinAtr). To date, however, the natural history of these subtypes, especially regarding the presence of subjects switching to other MRI patterns and their clinical and biological differences, remains poorly understood.

Objective: To investigate the clinical and biological underpinnings of longitudinal atrophy pattern progression in AD.

Methods: 251 AD patients (16 with significant memory concern, 66 with early mild cognitive impairment (MCI), 125 with late MCI, and 44 with AD dementia) from the Alzheimer's Disease Neuroimaging Initiative (ADNI) database were assigned to their baseline MRI atrophy subtype using Freesurfer-derived cortical:hippocampal volumes ratio. Switching to other MRI patterns was investigated on longitudinal scans, and patients were accordingly classified as "*switching*" and "*stable*". Logistic regression models were applied to identify predictors of switching to other MRI patterns.

Results: 40% of Lp, 26% of HpSp, and 35% of MinAtr cases switched to other MRI patterns, with tAD representing the destination subtype of all switching HpSp and Lp, and the majority of MinAtr. At baseline significant clinical, cognitive and biomarkers differences were observed across the four subtypes. Only clinical and cognitive variables, however, were significantly associated with switch to other MRI patterns.

Conclusions: Our results suggest convergent directions of disease progression across atypical and typical AD forms, at least in a subset of AD subjects, and highlight the importance of deep-phenotyping approaches to understand AD heterogeneity.

[1]IRCCS Ospedale Policlinico San Martino, Genoa, Italy
[2]Department of Health Sciences (DISSAL), University of Genoa, Genoa, Italy
[3]Department of Neuroscience, Rehabilitation, Ophthalmology, Genetics, Maternal and Child Health (DINOGMI), University of Genoa, Genoa, Italy
[4]Centre for Precision and Translational Medicine, Department of Medicine, Surgery and Neuroscience, University of Siena, Siena, Italy

[#]These authors contributed equally to this work as first authors.
[*]These authors contributed equally to this work as senior authors.

[§]Data used in preparation of this article were obtained from the Alzheimer's Disease Neuroimaging Initiative (ADNI) database (http://adni.loni.usc.edu). As such, the investigators within the ADNI contributed to the design and implementation of ADNI and/or provided data but did not participate in analysis or writing of this report. A complete listing of ADNI investigators can be found at: http://adni.loni.usc.edu/wp-content/uploads/how_to_apply/ADNI_Acknowledgement_List.pdf

Corresponding author:
Matteo Pardini, IRCCS Ospedale Policlinico San Martino and University of Genoa, Largo R. Benzi 10, 16132, Genoa, Italy.
Email: matteo.pardini@unige.it

Keywords
Alzheimer's disease, biomarkers, longitudinal study, magnetic resonance imaging, neuropathology

Received: 23 May 2024; accepted: 28 September 2024

Introduction

Recent years have seen a progressive increase in our understanding of the inter-individual differences in subjects with Alzheimer's disease (AD) and the need to develop easy-to-use and scalable approaches to evaluate *in vivo* the significant heterogeneity observed in this population.

A widely used approach is the recognition of different patterns of tissue damage distribution in AD and thus the characterization of patients across different clinical, pathological, and imaging subtypes.[1]

Regarding pathological data, for example, the presence of different patterns of cortical fibrillary tangles in post-mortem AD samples, has been leveraged to identify three distinct pathological subtypes: hippocampal sparing (HpSp), typical AD (tAD), and limbic predominant (Lp).[1]

More recently, it has been shown that it is relatively straightforward to identify in vivo these AD subtypes, using volumetric magnetic resonance imaging (vMRI) with a simple algorithmic approach based on the assessment of cortical volume (CV) and hippocampal volume (HVs). The identification of these subtypes has been shown to provide meaningful prognostic insights[2] and help the identification of subjects with higher probabilities of responding to symptomatic treatments.[3]

More recently, the use of vMRI has enabled the identification of a fourth subtype, the minimal atrophy (MinAtr) one,[4] with no or minimal signs of gray matter atrophy, but comparable baseline clinical severity relative to the other subtypes.[5]

Notably, while previous studies have investigated the longitudinal trajectories of clinical decline across these groups,[6] the possible switch of subtype over time in individual subjects and its association with clinical, cognitive, metabolic and cerebrospinal fluid (CSF) variables is still poorly characterized. Indeed, a key open question remains regarding the trajectories of atrophy progression across the different groups over time, and their biological determinants.

It is plausible to hypothesize that the different rates of clinical progression observed across the distinct MRI subtypes are not only influenced by the initial gray matter loss distribution but also by its longitudinal course of propagation.

Considering these observations, the aims of our study were: a) to confirm previous observations linking baseline MRI subtypes to distinct rates of clinical decline in AD, and b) to explore the **switch** from the baseline subtype to other MRI subtypes over time as well as its relationship with baseline and longitudinal clinical and biomarkers features.

Methods

Subject selection

Data used in the preparation of this article were obtained from the Alzheimer's Disease Neuroimaging Initiative (ADNI) database (http://adni.loni.usc.edu). The ADNI was launched in 2003 as a public-private partnership, led by Principal Investigator Michael W. Weiner, MD. The primary goal of ADNI has been to test whether serial magnetic resonance imaging (MRI), positron emission tomography (PET), other biological markers, and clinical and neuropsychological assessment can be combined to measure the progression of mild cognitive impairment (MCI) and early AD.

Inclusion criteria for our study were: a) a diagnosis of AD in the following clinical stages: dementia (ADD), MCI, or significant memory concern (SMC) as reported in ADNI procedures manuals, b) at least one positive amyloid biomarker based on amyloid PET imaging or CSF amyloid-β 1-42 ($A\beta_{1-42}$) according to ADNI procedure manuals and as previously described,[7] and c) baseline Freesurfer MRI data available (from the ADNI-1-2-GO datasets).

According to these criteria, we obtained an initial cohort of 266 patients. Among these, 15 were excluded due to a global segmentation failure in baseline Freesurfer MRI analyses (which in turn was related to extremely poor image quality, registration issues, or gross misestimation of the hippocampus).

The final cohort thus included 251 patients (16 SMC, 66 early MCI, 125 late MCI, and 44 ADD): 250 with available baseline CSF $A\beta_{42}$ values (of these patients, 160 also had available baseline AmyPET data) and 1 with only baseline AmyPET data.

As detailed below, for all the included patients the following variables were analyzed: a) demographic features, b) prevalence of *APOE* ϵ4, c) baseline clinical features, including age at symptoms onset, disease duration and clinical diagnosis d) baseline cognitive measures, and e) baseline markers of neurodegeneration including CSF total tau (tTau) and phosphorylated tau (pTau), the mean 18F-fluorodeoxyglucose (FDG)-PET hypometabolic convergence index (HCI), a measure of the severity of an AD-like hypometabolism pattern provided in the ADNI database,[8] and the AmyPET CSUVR.

Baseline clinical, cognitive, and genetic features

Following the ADNI protocol,[9] the MCI subjects were diagnosed with a Mini-Mental State Examination (MMSE) score between 24 and 30 and a Clinical Dementia Rating (CDR) of 0 or 0.5, with a memory box score of at least 0.5. The MCI subjects were also diagnosed with objective evidence of memory impairment, as determined by standardized memory tests, but with normal performance on other cognitive tests and preserved daily functioning.

The ADD subjects were diagnosed with an MMSE score between 20 and 26 and a CDR of 1 or higher. Subjects with ADD had to meet the criteria of the National Institute of Neurological and Communicative Disorders and Stroke—Alzheimer's Disease and Related Disorders Association for probable AD.

A delayed recall of one paragraph from the Logical Memory II subscale of the Wechsler Memory Scale—Revised (maximum score of 25) was used for the memory criterion with cutoff scores based on education as follows: normal subjects $\geq$9 for 16 years of education, $\geq$5 for 8–15 years of education, and $\geq$3 for 0–7 years of education. The scores for subjects with MCI and subjects with AD were $\leq$8 for 16 years of education, $\leq$4 for 8–15 years of education, and $\leq$2 for 0–7 years of education.

Baseline cognitive measures included the CDR-Sum of Boxes (CDR-SB), the MMSE, the Executive Function (EFCS) and Memory (MCS) composite scores.

APOE genotyping results were available on the ADNI repository and used as such. Briefly, *APOE* was performed using DNA extracted from peripheral blood cells that are collected in 1 EDTA plastic tube as previously described.[10]

CSF biomarkers

CSF sampling and processing were conducted by the ADNI protocol. CSF $A\beta_{1-42}$, t-tau, and p-tau_{181} were measured by Innogenetics/Fujirebio AlzBio3 immunoassay kits and the xMAPLuminex platform in the ADNI Biomarker Core laboratory at the University of Pennsylvania Medical Center.

PET biomarkers

Brain glucose metabolism was examined using FDG-PET. Details of the PET image processing protocol and generation of the HCI, a measure of the extent to which the pattern and magnitude of hypometabolism correspond to that observed in patients with a clinical diagnosis of AD, were previously published and are available online (https://adni.bitbucket.io/reference/baipetnmrc.html).8
Briefly, each participating site acquired and reconstructed the FDG-PET data with the use of measured-attenuation correction and the specified reconstruction algorithm for each scanner type according to a standardized protocol (http://www.loni.ucla.edu/ADNI/Data/ADNI_Data.shtml). All images were pre-processed by ADNI PET Coordinating Center investigators at the University of Michigan. The HCI is an individual-level metric that provides a single measurement of the extent to which a person's pattern and magnitude of cerebral hypometabolism correspond to that of AD. HC values are included in the outputs of ADNI already computed. Numerically the HCI is the voxel-by-voxel multiplication of the subject's hypometabolic map (based on the contrast between each patient and a healthy control group) and an average AD hypometabolic map based on a group of AD subjects, as described in Chen et al., 2011.[8] The HCI was computed as the voxel-wise summation across all the voxels at which z-scores from both maps were negative, divided by 10,000.

MRI analysis and patterns definition

Volumetric measures extracted with the Freesurfer image analysis suite available in the ADNI database (Freesurfer version 4.3 for ADNI 1, Freesurfer version 5.1 for ADNI 2-GO) were used. Using baseline MRI scans, all patients were initially classified as typical AD (tAD), hippocampal sparing (HpSp), limbic predominant (Lp), and minimal atrophy (MinAtr) according to the procedure previously described by Risacher and colleagues,[2] as follows: left and right gray matter volumes from lateral frontal (caudal and rostral midfrontal, pars opercularis, pars triangularis), superior temporal, and lateral parietal (inferior parietal, superior parietal, supramarginal) cortices in both cerebral hemispheres were summed to provide a composite measure of bilateral CV, while HVs were aggregated in a bilateral total HV.

Both the HV and CV measures were preadjusted for the effects of intracranial volume, scanner strength (1.5T versus 3T), age, and sex. The residual values for HV and CV were then used to calculate the HV:CV ratio and to split subjects in high and low HV and high and low CV volume using the median sample value as cut-off (respectively 6300 mm3 for the HV and 197000 mm3 for the CV).

Using the HV:CV ratio and the aforementioned split in high and low HV and CV volumes, all patients were stratified according to 4 different MRI patterns: typical AD (tAD), hippocampal sparing (HpSp), limbic predominant (Lp), and minimal atrophy (MinAtr). These patterns were defined using the two-step procedure described by Risacher and colleagues[2] and reported below.

From a qualitative point of view, Lp subjects were defined as those subjects with a more pronounced neurodegeneration in the hippocampus compared to the cortex, HpSp subjects those with a more pronounced neurodegeneration in the cortex compared to the hippocampus, tAD those with a significant but balanced neurodegeneration in both the cortex and the hippocampus and lastly MinAtr subjects as those without marked atrophy.

To this aim an algorithmic approach was proposed:

1. Participants with HV:CV ratios below the 25th percentile and both a high CV and low HV values were defined as Lp.
2. Participants with HV:CV ratios higher than the 75th percentile and both low CV and high HV values were as HpSp.
3. participants with HV:CV ratios between the 26th and the 74th percentiles and both low HV and low CV values were defined as tAD.
4. Participants with HV:CV ratios between the 26th and the 74th percentiles and both high HV and high CV values were defined as tAD.

Using longitudinal MRI scans, we further evaluated Freesurfer MRI volumetric metrics at each available follow-up visit until 24 months, excluding from the analyses all the MRI scans with global failure of segmentation (as performed for the baseline analyses).

We thus obtained a longitudinal cohort of 232 subjects: 177 subjects with both 12- and 24-month MRI scans available, 8 subjects with MRI scans available only at 12 months, and 47 subjects with MRI scans available only at 24 months.

Switch to other MRI patterns was then established using the same methodology applied for baseline MRI patterns definition (including the same cut-off values used at baseline for defining high and low HV and CV volume subjects), and patients in each group were therefore classified as "*switching*" and "*stable*".

Statistical analyses

Cross-sectional study. Continuous variables were compared between the four baseline MRI pattern groups using the Kruskal-Wallis test, and pairwise comparisons were subsequently tested using the post hoc Dunn test with Bonferroni correction for multiple comparisons. Categorical variables were compared using the chi-squared test.

Longitudinal study: Change in cognitive and MRI measures. Relative deltas of variation for all the investigated cognitive and MRI measures were calculated as the change between 12 months and baseline, and between 24 months and baseline. The deltas of variation were then compared between the four baseline MRI pattern groups using the Kruskal-Wallis test, and pairwise comparisons were subsequently tested using the post hoc Dunn test with Bonferroni correction for multiple comparisons.

Finally, linear mixed effects models with randomly varying intercepts and slopes were performed to assess pattern of changes over time in the four baseline MRI groups. Models were adjusted for gender and some transformations were done in case of skewed distributions. To evaluate patterns of change across groups we studied the overall interactions as well as the single comparisons between each baseline MRI group and tAD.

Longitudinal study: Switch to other MRI patterns. Baseline and longitudinal continuous variables were compared between "*switching*" and "*stable*" groups using the Mann-Whitney U test, while categorical variables were compared using the chi-squared test.

Afterward, we performed logistic regression models to identify significant predictors of switch to other MRI patterns among baseline variables, and to investigate significant associations between switching and longitudinal variables adjusting for the baseline MRI pattern. We also finally evaluated whether regression analyses results remained significant after further correction for gender.

For the deltas of variation of cognitive measures, results were reported as continuous as well as binary values, defining the optimal cut-point according to the Liu method, which maximizes the product of sensitivity and specificity.

All data were analyzed using Stata version 16.0 (Stata Corporation, College Station, TX, USA). Only results with p values < 0.05 were considered statistically significant.

Results

Cross-sectional findings

The overall prevalence of the distinct MRI patterns was 32% for tAD, 17% for Lp, 17% for HpSp, and 32% for MinAtr (Table 1).

As regards baseline clinical features, early MCI (eMCI) diagnoses were significantly less frequent in tAD compared to all the other groups and in HpSp compared to MinAtr, while late MCI (lMCI) was significantly more frequent in tAD than in MinAtr. AD diagnoses were more frequent in tAD patients compared to all the other MRI groups and in HpSp compared to MinAtr, while SMC was significantly less frequent in tAD and Lp compared to MinAtr (Table 1).

Concerning cognitive measures, CDR-SB scores were significantly higher in tAD and Lp compared to MinAtr as well as in tAD compared to HpSp. Similarly, all groups showed significantly lower MMSE scores compared to the MinAtr group, which presented overall higher MMSE performances (Table 1).

Significant differences were also observed for memory and executive function impairment. For memory significantly lower scores were observed in tAD compared to Lp, HpSp, and MinAtr and in Lp and HpSp compared to MinAtr (Table 1), while there were no significant differences in memory between Lp and HpSp subjects. Regarding the executive composite score, significantly lower scores were observed in tAD compared to Lp and MinAtr, and in HpSp compared to MinAtr (Table 1).

Table 1. Demographic, genetic and baseline clinical and biomarkers features of patient groups stratified by the baseline MRI pattern.

	tAD	Lp	HpSp	MinAtr
N	82	44	44	81
Demographic features				
Age	71.91 ± 6.88	72.68 ± 6.36	72.96 ± 8.27	73.61 ± 6.53
Gender [M/F]	**41/41**[a]	**33/11**[b, c, d]	**20/24**[a]	**43/38**[a]
Education [y]	15.81 ± 2.79	16.31 ± 3.04	15.84 ± 3.06	15.76 ± 2.83
Genetic features				
APOE ϵ4 [positive/negative]	61/21	35/9	29/15	59/22
Clinical features				
Age at symptoms onset	68.03 ± 6.36	67.69 ± 6.87	69.48 ± 8.80	69.91 ± 7.98
Disease duration at baseline [y]	3.86 ± 2.68	4.77 ± 3.74	2.97 ± 2.06	4.30 ± 3.69
Baseline diagnosis [eMCI/lMCI/ADD/SMC]	**6/48/28/0**[a, b, c]	**14/24/6/0**[c, d]	**10/24/7/3**[c, d]	**36/29/3/13**[a, b, d]
Cognitive measures				
CDR-SB	**2.78 ± 1.90**[b, c]	**1.97 ± 1.04**[c]	**1.86 ± 1.37**[d]	**1.25 ± 1.12**[a, d]
MMSE	**25.36 ± 2.69**[c]	**26.72 ± 2.20**[c]	**26.65 ± 2.14**[c]	**27.96 ± 1.95**[a, b, d]
EFCS	**−0.53 ± 0.89**[a, c]	**0.26 ± 0.80**[d]	**−0.16 ± 0.97**[c]	**0.36 ± 0.88**[b, d]
MCS	**−0.58 ± 0.53**[a, b, c]	**−0.20 ± 0.57**[c, d]	**−0.02 ± 0.62**[c, d]	**0.40 ± 0.64**[a, b, d]
Biomarkers features				
Amy PET CSUVR	1.43 ± 0.15	1.42 ± 0.15	1.43 ± 0.15	1.37 ± 0.16
HCI	**1.12 ± 0.12**[b, c]	**1.17 ± 0.08**[c]	**1.20 ± 0.14**[c, d]	**1.28 ± 0.13**[a, b, d]
CSF $A\beta_{42}$, pg/mL	**590.31 ± 175.99**[c]	613.93 ± 198.47	655.22 ± 166.48	**701.15 ± 183.81**[d]
CSF tTau, pg/mL	369.04 ± 133.07	378.81 ± 113.75	345.38 ± 111.70	330.93 ± 126.74
CSF pTau, pg/mL	37.03 ± 14.39	38.63 ± 12.57	35.48 ± 12.94	32.97 ± 13.86

Values are means ± standard deviations and absolute frequencies. [a]$p < 0.05$ compared to LpMRI, [b]$p < 0.05$ compared to HpSp, [c]$p < 0.05$ compared to MinAtr, [d]$p < 0.05$ compared to tAD.

AD: Alzheimer's disease; ADD: Alzheimer's disease dementia; Amy PET SUVR: Amyloid PET cortical standardized uptake value ratio; CDR-SB: Clinical Dementia Rating Scale sum of boxes; CSF: cerebrospinal fluid; EFCS: Executive function composite score; eMCI: early onset MCI; F: females; HCI: hypometabolic convergence index; HpSp: hippocampal sparing; lMCI: late onset MCI; Lp: limbic predominant; M: males; MCI: mild cognitive impairment; MCS: memory composite score; MMSE: Mini-Mental State Examination; MinAtr: minimal atrophy; pTau: phosphorylated tau; SMC: subjective memory complaint; tAD: typical AD; tTau: total tau.

Table 2. Longitudinal cognitive and MRI measures in patient groups stratified by the baseline MRI pattern.

	tAD	Lp	HpSp	Min Atr
N	74	43	38	77
Δ EFCS 12 months	−0.27 ± 0.53	−0.21 ± 0.60	−0.0002 ± 0.62	−0.03 ± 0.61
Δ EFCS 24 months	−0.54 ± 0.63[c]	−0.32 ± 0.81	−0.26 ± 0.82	−0.11 ± 0.69[d]
Δ MCS 12 months	−0.21 ± 0.35	−0.20 ± 0.29	−0.13 ± 0.37	−0.08 ± 0.32
Δ MCS 24 months	−0.38 ± 0.43[c]	−0.40 ± 0.38[c]	−0.31 ± 0.48[c]	−0.05 ± 0.46[d,a,b]
Δ CDR-SB 12 months	0.90 ± 1.44[c]	0.62 ± 1.02	0.43 ± 1.05	0.26 ± 1.12[d]
Δ CDR-SB 24 months	2.47 ± 2.22[c]	1.62 ± 1.53[c]	1.86 ± 1.82[c]	0.73 ± 1.49[d,a,b]
Δ MMSE 12 months	−2.32 ± 2.89[b,c]	−1.14 ± 2.17	−0.78 ± 2.74[d]	−0.33 ± 2.03[d]
Δ MMSE 24 months	−4.07 ± 3.90[c]	−3.37 ± 4.59[c]	−2.18 ± 3.52	−1.12 ± 4.01[a, d]
Δ CV 12 months	**−5099.30 ± 5611.71**	**−6807.03 ± 6957.24**	**−2517.37 ± 6360.48**	**−4609.22 ± 6356.78**
Δ CV 24 months	**−10291.15 ± 8393.42**[b,c]	**−9387.51 ± 8959.34**	**−5612.83 ± 8569.64**[d]	**−5570.23 ± 8200.79**[d]
Δ HV 12 months	**−246.59 ± 169.59**	**−230.22 ± 268.20**	**−222.39 ± 185.97**	**−204.14 ± 224.06**
Δ HV 24 months	**−498.79 ± 291.24**[c]	**−430.42 ± 327.61**	**−452.93 ± 270.36**	**−316.50 ± 315.17**[d]

Values are means ± standard deviations and absolute frequencies. [a]$p < 0.05$ compared to LpMRI, [b]$p < 0.05$ compared to HpSp, [c]$p < 0.05$ compared to MinAtr, [d]$p < 0.05$ compared to tAD.

AD: Alzheimer's disease; CDR-SB: Clinical Dementia Rating Scale sum of boxes; CV: cortical volume; Δ: delta of variation; EFCS: Executive function composite score; HpSp: hippocampal sparing; HV: hippocampal volume; Lp: limbic predominant; MCS: memory composite score; MMSE: Mini-Mental State Examination; MinAtr: minimal atrophy; tAD: typical AD.

As regards biomarkers, the [^{18}F] FDG PET HCI was significantly higher (thus more suggestive of AD) in MinAtr compared to all the other groups, and in HpSp compared to tAD. Lastly, CSF $A\beta_{42}$ was significantly higher in MinAtr compared to tAD while no significant differences were observed for Amy PET CSUVR and tau levels (both tTau and pTau) (Table 1).

Longitudinal findings

Longitudinal decline in cognitive and MRI measures. Longitudinal decline in cognitive and MRI measures at 12 and 24 months for each atrophy subtype are reported in Table 2. Among all the scales, the CDR-SB was the most able to detect differences between groups, with MinAtr subjects presenting with a more benign course compared to all other subtypes at 24 months, and to tAD subjects at 12 months. A similar pattern was also observed for the memory composite score, albeit only at 24 months, with MinAtr subjects showing a significantly more benign trajectory than all other groups. The executive composite score was not able to capture significant differences except for a more marked executive decline in tAD compared to MinAtr patients albeit only at the 24 months. The MMSE was the only scale able to capture differences between tAD, Lp and HpSp groups, with a significantly steeper decline in tAD compared to HsSp at 12 months, and to Lp subjects at 24 months.

With regards the decline in MRI measures, at 24 months tAD cases showed a steeper CV loss compared to HpSp and MinAtr patients, and a steeper HV loss compared to the MinAtr group.

The overall interaction evaluated using linear mixed effects models evidenced significant differences in EFCS, MFCS, CDR-SB, MMSE, CV, and HV patterns of change over time across baseline MRI subgroups (Figure 1).

In particular, single group comparisons between tAD and the other groups evidenced a significantly steeper MMSE decrease over time compared to MinAtr and HpSp patients; additional differences between the MinAtr and tAD groups were observed for the EFCS, MFCS, and CDR-SB patterns of change (Figure 1).

As regards the longitudinal decline in MRI features, tAD cases showed a steeper CV loss compared to both MinAtr and HpSp patients, and a steeper HV loss compared to MinAtr cases (Figure 1).

Switch to other MRI patterns over the follow-up period and associated features. Over the 24-month follow-up period, 40% of Lp cases (N=17) developed CV loss compatible with the tAD pattern while 60% of Lp patients (N=26) did not develop significant CV loss (Figure 2, Table 3). In the HpSp group, 26% of cases (N=10) progressively manifested HV loss compatible with the tAD pattern, while 74% of patients (N=28) did not develop HV loss (Figure 2, Table 3). In the MinAtr group 14% of cases (N=11) developed CV and HV loss compatible with the tAD pattern, 8% (N=6) progressively manifested HV loss compatible with the Lp pattern, 13% (N=10) developed CV loss compatible with the HpSp pattern and 65% (N=50) did not develop either CV or HV significant loss (Figure 2, Table 3).

We then examined the features associated with MRI subtype switch independently for each group, as reported in Table 3.

In the MinAtr group, switch to another atrophy subtype was associated with greater disease duration and severity (as assessed with the CDR-SB), a more diffuse FDG abnormalities pattern (i.e., a lower HCI index) and a higher PET amyloid burden.

Conversely, in Lp and HpSp groups, switch was associated only with longer symptoms duration (Lp) and more modest PET amyloid burden (HpSP).

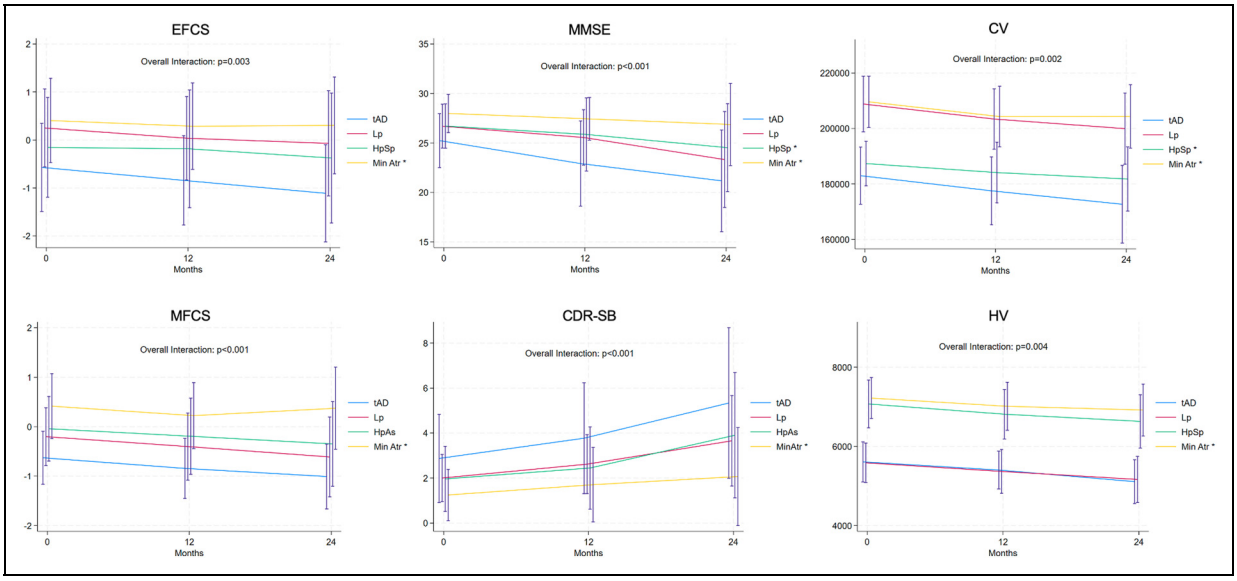

Figure 1. Longitudinal changes for key cognitive and MRI measures for the different MRI patterns.

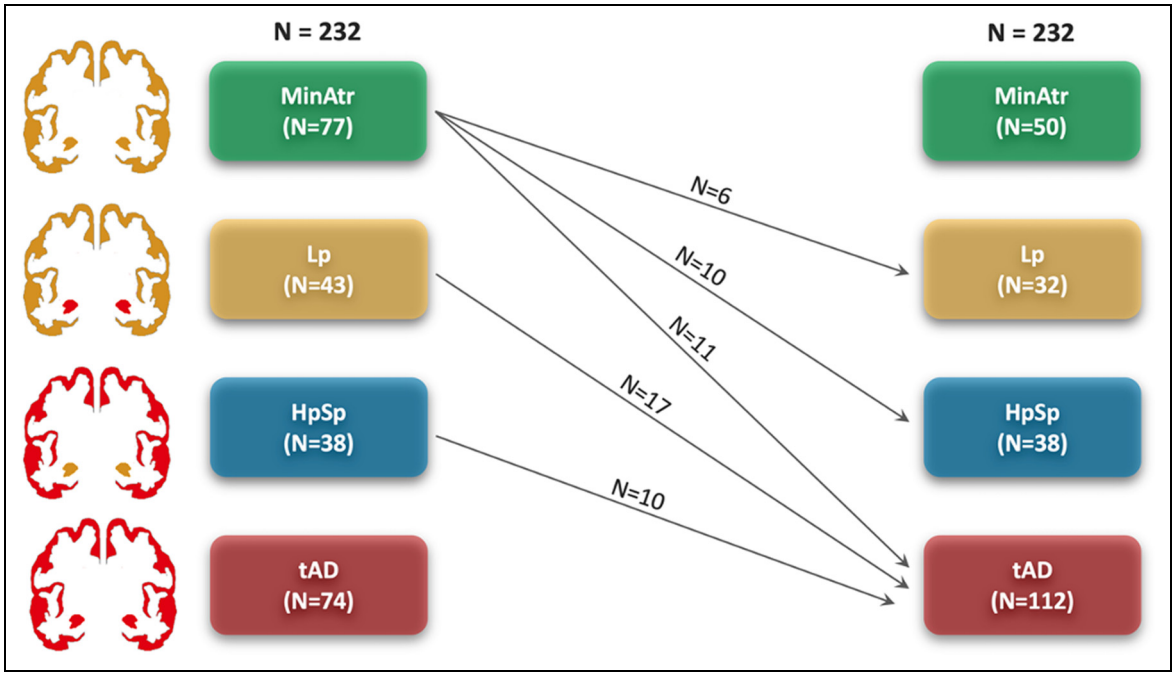

Figure 2. Switch across MRI patterns over the follow-up period.

Baseline predictors of switch to other MRI patterns and association with longitudinal clinical measures

As regards the role of demographic, genetic, biomarkers, and baseline clinical features in predicting the switch to other MRI patterns over the follow-up period, we observed that longer disease duration and greater CDR-SB scores were significant predictors of greater probability of switch to other MRI patterns (Table 4). Concerning longitudinal cognitive features, we found that greater decline in executive function at 24 months, memory at 12 and 24 months, and CDR-SB at 24 months were all significantly associated with greater probability of switch to other MRI patterns (Table 4). All the results remained significant after additional correction for gender.

Discussion

This study evaluated the biological underpinnings and the stability over time of the MRI atrophy subtypes in AD to better characterize their clinical relevance and enhance their possible clinical usefulness.

Cross-sectional study

The overall prevalence of the distinct MRI patterns observed in our study was comparable to that found in the original autopsy investigation[1] as well as in the most recent MRI studies[2,6] for Lp and HpSp cases, while we identified a slightly lower percentage of tAD patients and a significantly greater percentage of MinAtr cases possibly due to the additional inclusion, in our study, of SMC and MCI cases which in turn resulted in higher CV/HV cutpoints.

At baseline, significant differences were found across groups in multiple measures of disease severity and cognitive impairment, with tAD cases showing more severe impairment compared to all the other groups. In line with previous investigations,[4,6] the greatest differences were observed for CDR-SB and MMSE measures in the comparison between MinAtr and tAD cases. Both these measures provide a global assessment of cognition in AD and are often used as outcome measures in clinical trials.[11] This result is of relevance regarding the possible impact of the relative frequency of the different MRI patterns in clinical trials population on the observed cognitive outcomes and suggest the opportunity to conduct secondary analyses of clinical trials data based on atrophy subtypes.[12]

Concerning EFCS and MCS measures, the study by Risacher and co-workers observed a gradient of increasing executive impairment from HpSp to tAD and Lp groups, while no differences were detected in terms of memory deterioration.[2] Conversely, in our study, results from baseline EFCS and MCS analyses were in line with what could be expected based on the underlying neuroanatomical patterns of degeneration: groups characterized by greater isocortical atrophy performed worst on executive measures, while groups with greater hippocampal degeneration performed worst on memory evaluations. This difference is relevant regarding the need to develop composite cognitive markers in AD clinical trials with the aim to increase the sensibility of outcome cognitive markers.[12]

Table 3. Demographic, genetic, baseline and longitudinal features of MRI pattern groups stratified by the switching status.

	Lp		HpSp		Min Atr	
N	43		38		77	
	Switching	Stable	Switching	Stable	Switching	Stable
N	17	26	10	28	27	50
Baseline features						
Demographic features						
Age	72.23 ± 7.89	72.80 ± 5.35	71.07 ± 10.04	73.67 ± 8.07	74.25 ± 7.32	73.16 ± 6.26
Gender [M/F]	10/7	22/4	5/5	11/17	14/13	28/22
Education [y]	16.23 ± 2.90	16.46 ± 3.21	15.60 ± 2.63	15.78 ± 3.25	15.59 ± 2.51	16.12 ± 2.95
Genetic features						
APOE ϵ4 [positive/negative]	16/1	18/8	8/2	19/9	21/6	35/15
Clinical features						
Age at symptoms onset	65.41 ± 8.88	68.78 ± 5.59	70.28 ± 9.51	69.27 ± 9.24	69.47 ± 9.28	69.89 ± 7.27
Disease duration at baseline [y]	**6.37 ± 4.71***	3.83 ± 2.92	2.77 ± 2.66	3.18 ± 1.92	**5.89 ± 4.64***	3.50 ± 2.81
Baseline diagnosis [eMCI/lMCI/ADD/SMC]	2/11/4/0	11/13/2/0	2/7/1/0	7/12/6/3	12/12/1/2	22/15/2/11
CDR-SB	2.17 ± 0.93	1.88 ± 1.11	2.20 ± 1.33	1.87 ± 1.49	1.70 ± 1.41*	1.00 ± 0.88
MMSE	26.05 ± 2.51	27.11 ± 1.94	26.70 ± 2.05	26.71 ± 2.33	27.55 ± 2.13	28.22 ± 1.81
EFCS	0.29 ± 0.78	0.22 ± 0.84	0.27 ± 0.84	−0.30 ± 1.07	0.22 ± 0.81	0.50 ± 0.90
MCS	−0.33 ± 0.60	−0.11 ± 0.56	−0.003 ± 0.29	−0.05 ± 0.74	0.23 ± 0.50	0.51 ± 0.70
Biomarkers features						
Amy PET CSUVR	1.42 ± 0.13	1.41 ± 0.17	**1.31 ± 0.12***	1.47 ± 0.14	**1.43 ± 0.17***	1.34 ± 0.15
HCI	1.16 ± 0.10	1.17 ± 0.07	1.29 ± 0.13	1.18 ± 0.14	**1.24 ± 0.13***	1.31 ± 0.12
CSF $A\beta_{42}$, pg/mL	554.81 ± 181.48	655.25 ± 204.32	701.26 ± 139.68	639.40 ± 182.27	685.51 ± 192.67	717.40 ± 182.38
CSF tTau, pg/mL	369.81 ± 109.85	388.08 ± 118.23	368.76 ± 61.96	343.70 ± 128.77	353.35 ± 135.63	311.96 ± 117.06
CSF pTau, pg/mL	37.31 ± 12.27	39.87 ± 12.95	37.32 ± 7.81	35.41 ± 14.87	35.37 ± 15.24	30.90 ± 12.56
Longitudinal features						
Δ EFCS 12 months	**−0.44 ± 0.59***	−0.06 ± 0.57	0.25 ± 0.55	−0.09 ± 0.63	−0.19 ± 0.62	0.06 ± 0.60
Δ EFCS 24 months	**−0.76 ± 0.77***	−0.06 ± 0.73	−0.20 ± 1.00	−0.29 ± 0.77	**−0.35 ± 0.78***	0.03 ± 0.61
Δ MCS 12 months	**−0.33 ± 0.29***	−0.12 ± 0.27	−0.25 ± 0.34	−0.09 ± 0.38	−0.12 ± 0.33	−0.05 ± 0.31
Δ MCS 24 months	−0.54 ± 0.35	−0.32 ± 0.38	−0.40 ± 0.49	−0.27 ± 0.48	−0.14 ± 0.43	0.003 ± 0.47
Δ CDR-SB 12 months	**1.09 ± 0.94***	0.31 ± 0.96	−0.10 ± 1.10	0.63 ± 0.98	0.42 ± 1.34	0.16 ± 0.97
Δ CDR-SB 24 months	1.88 ± 1.48	1.46 ± 1.57	1.25 ± 1.50	2.10 ± 1.90	1.26 ± 1.93	0.43 ± 1.09
Δ MMSE 12 months	−1.18 ± 2.38	−1.12 ± 2.07	−1.10 ± 1.52	−0.67 ± 3.09	−0.36 ± 2.14	−0.31 ± 1.98
Δ MMSE 24 months	**−5.00 ± 6.39***	−2.31 ± 2.49	−2.00 ± 3.80	−2.25 ± 3.48	−0.93 ± 2.32	−1.22 ± 4.69

Values are means ± standard deviations and absolute frequencies. *$p < 0.05$ compared to non-progressors.

AD: Alzheimer's disease; ADD: Alzheimer's disease dementia; Amy PET SUVR: Amyloid PET cortical standardized uptake value ratio; CDR-SB: Clinical Dementia Rating Scale sum of boxes; CSF: cerebrospinal fluid; Δ: delta of variation; EFCS: Executive function composite score; eMCI: early onset MCI; F: females; HCI: hypometabolic convergence index; HpSp: hippocampal sparing; lMCI: late onset MCI; Lp: limbic predominant; M: males; MCI: mild cognitive impairment; MCS: memory composite score; MMSE: Mini-Mental State Examination; MinAtr: minimal atrophy; pTau: phosphorylated tau; SMC: subjective memory complaint; tAD: typical AD; tTau: total tau.

As regards the investigated biomarkers, published studies have reported heterogenous evidence regarding the association between MRI atrophy subtypes and AD core biomarkers, with some studies failing to detect any difference either in CSF or Amyloid PET measures between AD MRI subgroups,[2,6] and others (using different approaches to define MRI subtypes) showing higher levels of neurodegeneration assessed with total tau levels in HpSp subjects compared to tAD patients.[5] In our work, we confirmed the absence of significant differences for Amyloid PET SUVR values, but we observed significantly more pathological CSF $A\beta_{42}$ values in tAD compared to MinAtr cases, a finding which further confirms the association in the ADNI cohort of CSF AD markers with hippocampal involvement,[13] the key role of CSF markers in this population [7,8] and the observation of higher CSF $A\beta_{42}$ levels in MinAtr AD cases.[14]

The relative heterogeneity of the associations between the different atrophy subtypes and the core AD markers, suggests a key limitation of purely cross-sectional studies on the biological underpinnings of atrophy subtypes in AD (i.e., their inherent inability to capture the dynamics of atrophy switch in individual subjects across subtypes). A second key limitation of the correlations between atrophy subtypes and the core AD biomarkers is the

Table 4. Regression model linking baseline and longitudinal features of patients to probability of switching to another MRI pattern.

	OR (95%CI)	p	N^
Demographic features			
Age [10 years increase]	0.97 (0.60;1.55)	0.885	
Gender [female]	1.38 (0.69;2.74)	0.364	
Education	0.96 (0.86; 1.07)	0.454	
Genetic features			
APOE ϵ4 [positive]	2.18 (0.95; 5.01)	0.066	
Baseline features			
Clinical features			
Age at symptoms onset [10 years increase]	0.85 (0.52; 1.38)	0.502	118
Disease duration at baseline [5 years increase]	2.24 (1.23; 4.07)	0.008*	118
Baseline diagnosis			
ADD	1.00 (ref)	—	
eMCI	0.53 (0.16; 1.82)	0.316	
lMCI	1.11 (0.36; 3.47)	0.857	
SMC	0.19 (0.03; 1.20)	0.078	
Cognitive measures			
CDR-SB	1.44 (1.08; 1.92)	0.014*	
MMSE	0.86 (0.74; 1.01)	0.069	
EFCS	1.01 (0.69; 1.46)	0.971	
MCS	0.61 (0.35; 1.05)	0.073	
Biomarkers features			
Amy PET CSUVR	2.82 (0.26;30.12)	0.392	121
HCI	0.30 (0.02; 5.26)	0.409	146
CSF $A\beta_{42}$, pg/mL [100-units increase]	0.91 (0.76; 1.09)	0.316	157
CSF tTau, pg/mL [100-units increase]	1.16 (0.88; 1.53)	0.300	157
CSF pTau, pg/mL [10-units increase]	1.12 (0.87; 1.43)	0.389	157
Longitudinal features			
Δ EFCS 12			148
Continuous	0.65 (0.36; 1.15)	0.139	
>= 0.00†	0.82 (0.41;1.63)	0.564	
Δ EFCS 24			154
Continuous	0.51 (0.31; 0.82)	0.006*	
>=0.14†	0.75 (0.35;1.57)	0.443	
Δ MCS 12			148
Continuous	0.27 (0.09; 0.81)	0.020*	
>=−0.15†	0.45 (0.22;0.91)	0.027*	
Δ MCS 24			156
Continuous	0.41 (0.19; 0.92)	0.030*	
>=−0.18†	0.70 (0.34;1.44)	0.338	
Δ CDR-SB 12			146
Continuous	1.20 (0.87; 1.66)	0.272	
>=0.25†	1.56 (0.78;3.14)	0.212	
Δ CDR-SB 24			147
Continuous	1.15 (0.92; 1.42)	0.217	
>=1.25†	2.59 (1.21;5.52)	0.014*	
Δ MMSE 12			147
Continuous	0.97 (0.84; 1.13)	0.721	
>=−0.50†	0.60 (0.30; 1.19)	0.141	
Δ MMSE 24			
Continuous	0.97 (0.89; 1.05)	0.400	
>=−1.50†	0.66 (0.33;1.34)	0.251	

Values are odds ratios (95% confidence interval). *$p < 0.05$.

^ N reported only in case of missing values.

†Optimal cut-point according to the Liu method, which maximizes the product of sensitivity and specificity.

ADD: Alzheimer's disease dementia; Amy PET SUVR: Amyloid PET cortical standardized uptake value ratio; CDR-SB = Clinical Dementia Rating Scale sum of boxes; CI: confidence interval; CSF: cerebrospinal fluid; Δ: delta of variation; EFCS: Executive function composite score; eMCI: early onset MCI; HCI: hypometabolic convergence index; lMCI: late onset MCI; MCI: mild cognitive impairment; MCS: memory composite score; MMSE: Mini-Mental State Examination; OR: odds ratio; pTau: phosphorylated tau; SMC: subjective memory complaint; tTau: total tau.

known impact of other misfolded proteins such as TDP-43 and alpha-synuclein on the distribution of atrophy in AD subject. TDP-43, for example, has been shown to be associated with hippocampal sclerosis in subjects with Lp AD but not in the other pathological subtypes.[15] Regarding the association between alpha-synuclein and the atrophy subtypes, the published evidence is partly conflicting with pathological series showing an association between alpha-synuclein and thus Lewy bodies pathology with tAD and Lp cases[16] but also with HpSp[17] and with the pathological proxies of the MinAtr cases.[18] The heterogeneity of these reports suggests, from our point of view, the value of using a longitudinal approach to study MRI atrophy patterns in AD to try to better define the natural history of the different MRI subtypes and their heterogeneity over time.

Concerning the FDG-PET HCI, we confirmed previous observations of greater values in HpSp compared to Lp and tAD groups, but we further provided novel evidence that HCI is even more elevated in MinAtr cases. HCI is associated with the presence of a typical AD pattern of hypometabolism independent from atrophy,[8] thus its increased expression in subjects with more moderate atrophy confirms the role of FDG assessment as an early marker of cognitive impairment and its neural bases in AD.

Longitudinal study

When we compared the longitudinal trajectories of clinical decline across the distinct MRI subgroups, the greatest differences were observed over the 24-month follow-up period. At 12 months, indeed, only differences in CDR-SB and MMSE measures could be detected, with tAD showing a greater decline compared to MinAtr in the former measure and relative to both HpSp and MinAtr in the latter.

Conversely, at 24 months, different rates of deterioration between patient groups were evident across all the investigated clinical measures. In particular, the longitudinal trend of cognitive decline confirmed the pattern observed at baseline, with MinAtr cases performing better over time than tAD patients, and HpSp and Lp cases showing more impaired performances than MinAtr cases, respectively, in EFCS and MCS measures.

As stated above, the main novelty of our study is the focus on longitudinal patterns of atrophy progression as a marker of spreading pathology across the distinct AD MRI subtypes.

Overall, our analysis suggests that the transition between different atrophy groups is somewhat ordered with a directionality from the MinAtr pattern to the tAD group. This hypothesis is based on the transitions observed in the study, and it is supported by the differences in the explored biomarkers reported in the paper as well as, more broadly, by the cut-off based approach used to define the different MRI groups.

Over the study period, about a third of Lp and HpSp patients switched to the tAD pattern. Intriguingly, in the MinAtr group, the observed patterns of longitudinal atrophy switch were more heterogeneous, with 14% of cases switching to the tAD pattern, 8% to the Lp pattern, and 13% to the HpSp pattern.

The relative instability over time of the MinAtr classification suggests that at least in a subset of subjects this may represent an earlier phase of the clinically-overt disease process associated with multiple possible trajectories of evolution to either typical or atypical disease forms. From a pathological point of view the MinAtr subjects are those with the more heterogenous pathological underpinnings and this mirrors the longitudinal findings of our study (i.e., the possible switch of MinAtr subjects to tAD, HpSp or Lp). As previously reported, indeed, the MinAtr subtype has been associated with both higher[18] and lower[19] frequencies of alpha-synuclein pathological inclusions than tAD subjects, thus highlighting the need of longitudinal MRI assessments to characterize the different populations included in the MinAtr group.

Notably, those MinAtr subjects who switched to another MRI subtype presented, at baseline, with a higher amyloid load and a less evident FDG pattern in absence of differences in cognitive performance or reserve compared to those who remained stable.

This observation suggests that at least in those MinAtr cases remaining stable, functional abnormalities may represent the neural bases of the cognitive abnormalities observed in absence of significant cortical atrophy. In a recent resting state fMRI study, indeed, diffuse functional connectivity abnormalities of the three main posterior brain networks (fronto-parietal, visual, and default-mode) were observed in MinAtr cases.[20] Conversely, the lack of significant differences in cognitive reserve (as assessed with education) between MinAtr and the other MRI subtypes, or between switching and stable MinAtr subjects, suggests that the cognitive reserve paradigm alone does not provide a significant explanation for the discrepancy between cognitive performance and gray matter volume in MinAtr cases.

A key result of our study is the characterization of the differences between *switching* and *stable* patients in each MRI subgroup, which is of relevance both regarding the natural history of the different atrophy subtypes and the clinical and biological heterogeneity of each subgroup. Indeed, our data suggest that at least in the *switching* subgroup, the tAD pattern seems to represent a final common destination for subjects previously presenting with any of the other MRI patterns.

Indeed, when we examined, in the whole sample, the contribution of clinical features to the probability of switching to other MRI patterns over the study period, we found

that significant predictors of a greater probability of switch included longer disease duration and higher CDR-SB at baseline. Additionally, steeper cognitive decline was further associated with MRI patterns switch.

The predictive role of the identified variables is in line with the main hypothesis of our work, specifically, that switching to other MRI patterns may represent a valuable proxy of spreading neurodegeneration in AD which, in turn, is by definition influenced by the disease time course and is related to progressive clinical and functional deterioration.

Also the lack of switch across atrophy subtypes in the majority of subjects, albeit in the limited time frame of this study, is of clinical significance. Indeed, recent studies showed that the atrophy pattern is related to the response to symptomatic therapies with cholinergic inhibitors, with a more marked response in those subjects with a MinAtr pattern.[3] In this context, a greater knowledge of the longitudinal trajectories of progression, as well as a more accurate characterization of *switching* cases might be particularly useful to accelerate personalized medicine approaches to AD treatment, as well as to guide clinical trials design especially regarding the use of MRI metrics as surrogate markers.

Additionally, while our finding of heterogeneous clinical stages within each MRI subtype argues against the hypothesis that the diverse atrophy patterns simply reflect similar damage distribution in different AD clinical stages, a thorough analysis of the association between temporal atrophy progression and clinical AD stages would be a key advance in knowledge deserving future investigation.

Finally, an intriguing aspect requiring further research is the association between age and MRI patterns of atrophy. While aging is indeed a well-known driver of atrophy, in our study we did not observe significant age differences between MRI subtypes, as well as between switching and stable cases. This finding was further corroborated by the regression analysis looking at the probability of switching to another MRI pattern, where age did not result as a significant predictor. While this phenomenon might be due to the fact that the MRI patterns were mainly defined based on the initial regional distribution of atrophy (less dependent on age) rather than only on its severity (more dependent on age), future research is required to fully elucidate this aspect.

In conclusion, by evaluating longitudinal patterns of atrophy progression across the main AD MRI subtypes and evaluating its association with clinical and biomarker measures, our study provides novel insights into AD spreading pathology. The obtained results suggest heterogeneous onset features but also convergent directions of pathological propagation across atypical and typical AD forms, and highlight the importance of deep-phenotyping approaches embedding clinical, genetic, and biomarker data to predict pathology evolution in AD.

Acknowledgments

Data collection and sharing for this project was funded by the Alzheimer's Disease Neuroimaging Initiative (ADNI) (National Institutes of Health Grant U01 AG024904) and DOD ADNI (Department of Defense award number W81XWH-12-2-0012). ADNI is funded by the National Institute on Aging, the National Institute of Biomedical Imaging and Bioengineering, and through generous contributions from the following: AbbVie, Alzheimer's Association; Alzheimer's Drug Discovery Foundation; Araclon Biotech; BioClinica, Inc.; Biogen; Bristol-Myers Squibb Company; CereSpir, Inc.; Cogstate; Eisai Inc.; Elan Pharmaceuticals, Inc.; Eli Lilly and Company; EuroImmun; F. Hoffmann-La Roche Ltd and its affiliated company Genentech, Inc.; Fujirebio; GE Healthcare; IXICO Ltd; Janssen Alzheimer Immunotherapy Research & Development, LLC.; Johnson & Johnson Pharmaceutical Research & Development LLC.; Lumosity; Lundbeck; Merck & Co., Inc.; Meso Scale Diagnostics, LLC.; NeuroRx Research; Neurotrack Technologies; Novartis Pharmaceuticals Corporation; Pfizer Inc.; Piramal Imaging; Servier; Takeda Pharmaceutical Company; and Transition Therapeutics. The Canadian Institutes of Health Research is providing funds to support ADNI clinical sites in Canada. Private sector contributions are facilitated by the Foundation for the National Institutes of Health (http://www.fnih.org). The grantee organization is the Northern California Institute for Research and Education, and the study is coordinated by the Alzheimer's Therapeutic Research Institute at the University of Southern California. ADNI data are disseminated by the Laboratory for Neuro Imaging at the University of Southern California.

ORCID iDs

Pilar M. Ferraro https://orcid.org/0000-0002-5008-2791
Laura Filippi https://orcid.org/0009-0007-8539-9565
Marta Ponzano https://orcid.org/0000-0003-4091-4686
Beatrice Orso https://orcid.org/0000-0001-9983-7940
Andrea Brugnolo https://orcid.org/0000-0002-5708-0940
Matteo Pardini https://orcid.org/0000-0002-4740-1982

Statements and declarations

Author contributions

Pilar Maria Ferraro (Conceptualization; Formal analysis; Methodology; Writing – original draft; Writing – review & editing); Laura Filippi (Conceptualization; Formal analysis; Writing – original draft; Writing – review & editing); Marta Ponzano (Formal analysis; Methodology; Writing – original draft; Writing – review & editing); Alessio Signori (Formal analysis; Methodology; Writing – original draft; Writing – review & editing); Beatrice Orso (Conceptualization; Investigation; Writing – original draft; Writing – review & editing); Federico Massa (Investigation; Writing – original draft; Writing – review & editing); Dario Arnaldi (Investigation; Writing – original draft; Writing – review & editing); Stefano Caneva (Investigation; Writing – original draft; Writing – review &

editing); Lucia Argenti (Investigation; Writing – original draft; Writing – review & editing); Mattia Losa (Investigation; Writing – original draft; Writing – review & editing); Lorenzo Lombardo (Investigation; Writing – original draft; Writing – review & editing); Pietro Mattioli (Investigation; Writing – original draft; Writing – review & editing); Mauro Costagli (Investigation; Writing – original draft; Writing – review & editing); Lorenzo Gualco (Investigation; Writing – original draft; Writing – review & editing); Martina Pulze (Investigation; Writing – original draft; Writing – review & editing); Domenico Plantone (Investigation; Writing – original draft; Writing – review & editing); Andrea Brugnolo (Investigation; Writing – original draft; Writing – review & editing); Nicola Girtler (Investigation; Writing – original draft; Writing – review & editing); Andrea Diociasi (Investigation; Writing – original draft; Writing – review & editing); Sara Garbarino (Investigation; Writing – original draft; Writing – review & editing); Flavio Villani (Investigation; Writing – original draft; Writing – review & editing); Maria Pia Sormani (Investigation; Writing – original draft; Writing – review & editing); Antonio Uccelli (Funding acquisition; Supervision; Writing – original draft; Writing – review & editing); Luca Roccatagliata (Conceptualization; Funding acquisition; Supervision; Writing – original draft; Writing – review & editing); Matteo Pardini (Conceptualization; Funding acquisition; Supervision; Writing – original draft; Writing – review & editing).

Funding

The authors disclosed receipt of the following financial support for the research, authorship, and/or publication of this article: Work supported by: #NEXTGENERATIONEU (NGEU) and funded by the Ministry of University and Research (MUR), National Recovery and Resilience Plan (NRRP), project MNESYS (PE0000006) – (DN. 1553 11.10.2022) and project RAISE (ECS00000035) – (DN. 1053 del 23.06.2022); the Italian Ministry of Research, under the complementary actions to the NRRP "Fit4MedRob - Fit for Medical Robotics" Grant (# PNC0000007); Italian Ministry of Health "Fondi per la Ricerca Corrente 2022-2024" to IRCCS Ospedale Policlinico San Martino; grant number NET-2018-12366666 NeuroArtP3 from the Italian Ministry of Health.

Declaration of conflicting interests

The authors declared the following potential conflicts of interest with respect to the research, authorship, and/or publication of this article: Federico Massa is an Editorial Board Member of this journal but was not involved in the peer-review process of this article nor had access to any information regarding its peer-review. The remaining authors declared no potential conflicts of interest with respect to the research, authorship, and/or publication of this article.

Data availability

The data set is owned by the Alzheimer's Disease Neuroimaging Initiative (ADNI). Data are publicly and freely available from the http://adni.loni.usc.edu/data-samples/access-data/ Institutional Data Access / Ethics Committee (contact via http://adni.loni.usc.edu/data-samples/access-data/) upon sending a request that includes the proposed analysis and the named lead investigator.

References

1. Murray ME, Graff-Radford NR, Ross OA, et al. Neuropathologically defined subtypes of Alzheimer's disease with distinct clinical characteristics: a retrospective study. *Lancet Neurol* 2011; 10: 785–796.
2. Risacher SL, Anderson WH, Charil A, et al. Alzheimer disease brain atrophy subtypes are associated with cognition and rate of decline. *Neurology* 2017; 89: 2176–2186.
3. Diaz-Galvan P, Lorenzon G, Mohanty R, et al. Differential response to donepezil in MRI subtypes of mild cognitive impairment. *Alzheimers Res Ther* 2023; 15: 117.
4. Byun MS, Kim SE, Park J, et al. Heterogeneity of regional brain atrophy patterns associated with distinct progression rates in Alzheimer's disease. *PLoS One* 2015; 10: e0142756.
5. Ferreira D, Nordberg A and Westman E. Biological subtypes of Alzheimer disease: a systematic review and meta-analysis. *Neurology* 2020; 94: 436–448.
6. Ferreira D, Verhagen C, Hernández-Cabrera JA, et al. Distinct subtypes of Alzheimer's disease based on patterns of brain atrophy: longitudinal trajectories and clinical applications. *Sci Rep* 2017; 18: 46263.
7. Kang JH, Korecka M, Figurski MJ, et al. The Alzheimer's disease neuroimaging initiative 2 biomarker core: a review of progress and plans. *Alzheimers Dement* 2015; 11: 772–791.
8. Chen K, Ayutyanont N, Langbaum JBS, et al. Characterizing Alzheimer's disease using a hypometabolic convergence index. *Neuroimage* 2011; 56: 52–60.
9. Petersen RC, Aisen PS, Beckett LA, et al. Alzheimer's Disease Neuroimaging Initiative (ADNI): clinical characterization. *Neurology* 2010; 74: 201–209.
10. Crook R, Hardy J and Duff K. Single-day apolipoprotein E genotyping. *J Neurosci Methods* 1994; 53: 125–127.
11. Cedarbaum JM, Jaros M, Hernandez C, et al. Rationale for use of the clinical dementia rating sum of boxes as a primary outcome measure for Alzheimer's disease clinical trials. *Alzheimers Dement* 2013; 9: 45–55.
12. Shand C, Markiewicz PJ, Cash DM, et al. Heterogeneity in preclinical Alzheimer's disease trial cohort identified by image-based data-driven disease progression modelling. medRxiv 2023. doi: 10: 2023.02.07.23285572. [Preprint]. Posted February 10, 2023.
13. Apostolova LG, Hwang KS, Andrawis JP, et al. 3D PIB and CSF biomarker associations with hippocampal atrophy in ADNI subjects. *Neurobiol Aging* 2010; 31: 1284–1303.
14. Persson K, Eldholm RS, Barca ML, et al. MRI-assessed atrophy subtypes in Alzheimer's disease and the cognitive reserve hypothesis. *PLoS One* 2017; 12: e0186595.
15. Josephs KA, Whitwell JL, Tosakulwong N, et al. TAR DNA-binding protein 43 and pathological subtype of Alzheimer's disease impact clinical features. *Ann Neurol* 2015; 78: 697–709.

16. Janocko NJ, Brodersen KA, Soto-Ortolaza AI, et al. Neuropathologically defined subtypes of Alzheimer's disease differ significantly from neurofibrillary tangle-predominant dementia. *Acta Neuropathol* 2012; 124: 681–692.
17. Jellinger KA. Neuropathological subtypes of Alzheimer's disease. *Acta Neuropathologica* 2012; 123: 153–154.
18. Boon BDC, Labuzan SA, Peng Z, et al. Retrospective evaluation of neuropathologic proxies of the minimal atrophy subtype compared with corticolimbic Alzheimer disease subtypes. *Neurology* 2023; 101: e1412–e1423.
19. Mohanty R, Ferreira D, Frerich S, et al. Neuropathologic features of antemortem atrophy-based subtypes of Alzheimer disease. *Neurology* 2022; 99: e323–e333.
20. Ferreira D, Pereira JB, Volpe G, et al. Subtypes of Alzheimer's disease display distinct network abnormalities extending beyond their pattern of brain atrophy. *Front Neurol* 2019; 28: 524.